Cardiovascular Research (2011) **89**, 290–299
doi:10.1093/cvr/cvq333

Globotriaosylceramide leads to $K_{Ca}3.1$ channel dysfunction: a new insight into endothelial dysfunction in Fabry disease

Seonghee Park[1], Ji Aee Kim[1], Ka Young Joo[1], Shinkyu Choi[1], Eun-Nam Choi[2], Jung-A. Shin[3], Ki-Hwan Han[3], Sung-Chul Jung[2], and Suk Hyo Suh[1]*

[1]Department of Physiology, School of Medicine, Ewha Womans University, 911-1 Mok-6-dong, Yang Chun-gu, Seoul 158-710, Republic of Korea; [2]Department of Biochemistry, School of Medicine, Ewha Womans University, Seoul, Republic of Korea; and [3]Department of Anatomy, School of Medicine, Ewha Womans University, Seoul, Republic of Korea

Received 23 June 2010; revised 11 October 2010; accepted 18 October 2010; online publish-ahead-of-print 21 October 2010

Time for primary review: 20 days

Aims Excessive endothelial globotriaosylceramide (Gb3) accumulation is associated with endothelial dysfunction and impaired endothelium-dependent relaxation in Fabry disease. In endothelial cells, $K_{Ca}3.1$ channels contribute to endothelium-dependent relaxation. However, the effect of Gb3 on $K_{Ca}3.1$ channels and the underlying mechanisms of Gb3-induced dysfunction are unknown. Herein, we hypothesized that Gb3 accumulation induces $K_{Ca}3.1$ channel dysfunction and aimed to clarify the underlying mechanisms.

Methods and results The animal model of Fabry disease, α-galactosidase A (*Gla*) knockout mice, displayed age-dependent $K_{Ca}3.1$ channel dysfunction. $K_{Ca}3.1$ current and the channel expression were significantly reduced in mouse aortic endothelial cells (MAECs) of aged *Gla* knockout mice, whereas they were not changed in MAECs of wild-type and young *Gla* knockout mice. In addition, $K_{Ca}3.1$ current and the channel expression were concentration-dependently reduced in Gb3-treated MAECs. In both Gb3-treated and aged *Gla* knockout MAECs, extracellular signal-regulated kinase (ERK) and activator protein-1 (AP-1) were down-regulated and repressor element-1 silencing transcription factor (REST) was up-regulated. Gb3 inhibited class III phosphoinositide 3-kinase and decreased intracellular levels of phosphatidylinositol 3-phosphate [PI(3)P]. In addition, endothelium-dependent relaxation was significantly attenuated in Gb3-treated mouse aortic rings.

Conclusion Gb3 accumulation reduces $K_{Ca}3.1$ channel expression by down-regulating ERK and AP-1 and up-regulating REST and the channel activity by decreasing intracellular levels of PI(3)P. Gb3 thereby evokes $K_{Ca}3.1$ channel dysfunction, and the channel dysfunction in vascular endothelial cells may contribute to vasculopathy in Fabry disease.

Keywords α-Galactosidase A knockout mice • Endothelial dysfunction • Fabry disease • Globotriaosylceramide • $K_{Ca}3.1$ channel

1. Introduction

Fabry disease (OMIM #301500) is an X-linked recessive metabolic disorder that arises secondary to the deficiency of lysosomal α-galactosidase A (*Gla*), resulting in an excessive accumulation of globotriaosylceramide (Gb3) in the vascular endothelium in multiple organs of the body, including the skin, kidneys, brain, and cardiovascular system.[1,2] The excessive vascular endothelial accumulation of Gb3 is implicated in endothelial dysfunction in Fabry patients as well as *Gla* knockout mice, an animal model of Fabry disease. According to clinical studies, endothelial dysfunction is the common manifestation of various cardiovascular diseases that are predominantly responsible for premature mortality in Fabry patients around the fourth to fifth decade of life.[3,4] In addition, several studies have demonstrated endothelial dysfunction in *Gla* knockout mice. In aged *Gla* knockout mice, the expression of endothelial nitric oxide synthase (eNOS) is significantly decreased and endothelium-dependent relaxation (EDR) is also impaired compared with that of age-matched wild-type mice, suggesting progressive Gb3 accumulation evokes endothelial dysfunction.[5,6]

Various cellular functions are modulated by ion channels. The intermediate-conductance Ca^{2+}-activated K^+ ($K_{Ca}3.1$) channel contributes to EDR through the modulation of the electrochemical

* Corresponding author. Tel: +82 2 2650 5722; fax: +82 2 2653 7891, Email: shsuh @ewha.ac.kr

driving force for Ca^{2+} entry[7] and plays a significant role in the regulation of vascular tone; this suggests that K_{Ca}3.1 channel dysfunction may cause endothelial dysfunction and thereby vascular disease.[8] In addition, sphingolipids can produce cellular dysfunction by affecting ion channels. Ceramide down-regulated the HERG K^+ channel in HEK 293 cells, and sphingosine inhibited voltage-operated Ca^{2+} channels in GH4C1 cells.[9,10] Therefore, endothelial dysfunction, which is found in *Gla* knockout mice, may be caused by Gb3-induced K_{Ca}3.1 channel dysfunction. However, it is unknown whether Gb3 accumulation evokes K_{Ca}3.1 channel dysfunction.

Our data show that Gb3 induces K_{Ca}3.1 channel dysfunction and thereby inhibits endothelial function. K_{Ca}3.1 channel dysfunction is caused by at least two mechanisms: down-regulation of K_{Ca}3.1 channels and inhibition of K_{Ca}3.1 channel activity. Gb3 down-regulates K_{Ca}3.1 channel via inhibition of the extracellular signal-regulated kinase (ERK)/activator protein-1 (AP-1) pathway and up-regulation of repressor element-1 silencing transcription factor (REST), and inhibits the current by decreasing intracellular phosphatidylinositol 3-phosphate [PI(3)P] concentrations. These results explain the underlying mechanisms of endothelial dysfunction in Fabry disease.

2. Methods

2.1 Animals and cell culture

A pair of Fabry mice, kindly provided by Dr Roscoe O. Brady of the National Institutes of Health (Bethesda, MD, USA), was bred to acquire a sufficient number of mice for this study. All mice were genotyped using PCR as described previously.[11] A minimum of 3 age-matched mice were used for each group. Mice were fed an autoclaved diet and water *ad libitum*. All mice were treated in accordance with the Animal Care Guidelines of the Ewha Womans University, School of Medicine and the National Institutes of Health Guide for the Care and Use of Laboratory Animals.

Mouse aortic endothelial cells (MAECs) were isolated from mice as described[12,13] and 1,1′-dioctadecyl-3,3,3′,3′-tetramethyl-indocarbocyanine perchlorate (DiI)-labelled acetylated low-density lipoprotein (DiI-Ac-LDL; Biomedical Technologies, Inc., Stoughton, MA, USA) uptake was used to demonstrate the endothelial nature from the isolated cells.

2.2 Electrophysiology

Electrophysiological methods have been described in detail elsewhere.[14] In short, whole-cell currents were measured using ruptured patches. Currents were monitored in voltage-clamp modes with an EPC-9 (HEKA Elektronik, Lambrecht, Germany). The holding potential of the whole-cell experiment was 0 mV, and currents were monitored during agonist stimulation by the repetitive application of 650 ms voltage ramps from −100 to + 100 mV (sampling interval 0.5 ms, 10 s intervals between ramps).

The standard external solution contained (in mmol/L): 150 NaCl, 6 KCl, 1.5 $CaCl_2$, 1 $MgCl_2$, 10 HEPES, 10 glucose, pH adjusted to 7.4 with NaOH. The pipette solution for whole-cell recording contained (in mmol/L): 40 KCl, 100 K-aspartate, 2 $MgCl_2$, 0.1 EGTA, 4 Na_2ATP, 10 HEPES, pH adjusted to 7.2 with KOH. For buffering free Ca^{2+}, the appropriate amount of Ca^{2+} was added in the presence of 5 mmol/L EGTA. K_{Ca}3.1 currents were normalized to cell capacitance and TRAM-34-sensitive current was measured as K_{Ca}3.1 current.

2.3 Contraction measurement on isolated aortic rings

Five to six-month-old mice were anaesthetized by an intraperitoneal injection of pentobarbital sodium (50 mg/kg body weight). The thoracic aorta was dissected out and cut into rings of about 3 mm. Mechanical responses were recorded from the aortic ring segments using a home-made myograph. Each aortic ring was threaded with two strands of tungsten wire (120 μm in diameter). One wire was anchored in the organ bath chamber (1 mL) and the other was connected to a mechano-transducer (Grass, FT-03) mounted on a three-dimensional manipulator. The muscle chamber was perfused at a flow rate of 2.5 mL/min with oxygenated (95% O_2/5% CO_2) Krebs/Ringer bicarbonate solution with a peristaltic pump. The composition (in mmol/L) of the Krebs solution was NaCl 118.3, KCl 4.7, $MgCl_2$ 1.2, KH_2PO_4 1.22, $CaCl_2$ 2.5, $NaHCO_3$ 25.0, glucose 11.1, pH 7.4. Rings were precontracted with 1 μmol/L U46619 and EDR was induced by acetylcholine (ACh).

2.4 Real-Time PCR and immunoblot analysis

RNA isolation was performed using the RNeasy Mini Kit (Qiagen, Valencia, CA, USA), and RNA was then reverse transcribed using a High Capacity cDNA Archive Kit (Applied Biosystems, Foster City, CA, USA). PCRs were performed on an ABI 7000 sequence detection system (Applied Biosystems) using a SYBR Green PCR Master Mix (Applied Biosystems). Primers for the mouse K_{Ca}3.1 channel gene (*Kcnn4*) were 5′-AAGCACACTCGAAGGAAGGA-3′ (sense) and 5′-CCGTCGATTCT CTTCTCCAG-3′ (antisense), and primers for the mouse REST gene (*Rest*) were 5′- GTGCGAACTCACACAGGAGA-3′ (sense) and 5′-AAG AGGTTTAGGCCCGTTGT-3′ (antisense). mRNA expression was normalized to the house-keeping gene, mouse *Gapdh* (5′-TCCATGACAACTTT GGCATTG-3′ (sense) and 5′-TCACGCCACAGCTTTCCA-3′ (antisense).

For immunoblot analysis, 30 μg of protein from cell homogenates was subjected to sodium dodecyl sulfate polyacrylamide gel electrophoresis (7.5–12% gels), and proteins were then transferred to a nitrocellulose membrane. Membranes were blocked for 1 h with TBST (10 mmol/L Tris–HCl, 150 mmol/L NaCl, and 1% Tween 20, pH 7.6) containing 5% bovine serum albumin at room temperature. The blots were incubated for 3 h with primary antibody against primary K_{Ca}3.1 antibody (IK1; Santa Cruz Biotechnology, Santa Cruz, CA, USA), p-ERK (Cell Signaling Technology, Beverly, MA, USA), or Class III phosphoinositide 3-kinase (PI3K; Cell Signaling Technology), followed by incubation with horseradish peroxidase-conjugated secondary antibodies for 1 h. Bands were visualized by chemiluminescence. Data collection and processing were performed using a luminescent image analyzer LAS-3000 and Image Gauge software (Fuji-Film, Tokyo, Japan).

2.5 Electrophoretic mobility shift assay (EMSA)

EMSAs were performed using a double-stranded oligonucleotide for AP-1 (5′-CTGCGCTTGATGACTCAGCAGCCGGA-3′). For the binding reaction, nuclear protein extract (10 μg) was incubated in a total volume of 20 μL in a binding buffer containing 10 mmol/L HEPES, pH 7.5, 5% glycerol, 50 mmol/L KCl, 1 mmol/L dithiothreitol, and 1 μg poly (dI-dC), and radiolabelled DNA (about 40 000 cpm) for 30 min at room temperature. DNA–protein complexes were resolved in a pre-electrophoresed 6% non-denaturing polyacrylamide gel at 4°C. Subsequently, the gel was dried under vacuum and exposed to film.

2.6 Fluorescence confocal microscopy

MAECs were grown on glass coverslips precoated with 1% gelatin and incubated in growth medium containing 10 μg/mL of DiI-Ac-LDL at 37°C for 4 h. After washing with PBS to remove free DiI-Ac-LDL, cells were fixed with 3.7% paraformaldehyde, permeabilized with 0.25% Triton X-100, and blocked for 1 h at room temperature in PBS with 10% BSA. After washing, cells were incubated overnight at 4°C with a diluted (1:50) primary K_{Ca}3.1 antibody, washed again and incubated for 1 h at room temperature with a secondary antibody, Alexa Flour 555 donkey anti-goat IgG (1:1500; Molecular probes, Eugene, OR, USA). After that, the cells were counterstained with 4′,6-diamidino-2-phenylindole dihydrochloride (DAPI). The mounted coverslips were viewed under a confocal microscope (Carl Zeiss, Gottingen, Germany) and photographed as described previously.[15]

2.7 Tissue preservation and immunohistochemistry

The abdominal aorta and inferior vena cava were removed and fixed by immersion in a periodate-lysine-2% paraformaldehyde solution overnight at 4°C. Tissues were cut transversely into 1 to 2 mm thick slices and processed for immunohistochemical studies using a horseradish peroxidase technique. Slices of tissue were embedded in paraffin.

Four-micrometer sections were deparaffinized with xylene and hydrated in a graded series of ethanol. After rinsing in tap water, sections were incubated with 3% H_2O_2 for 30 min to eliminate endogenous peroxidase activity. The sections were treated with blocking serum for 30 min and incubated overnight at 4°C in primary $K_{Ca}3.1$ antibody. After being washed in PBS, the sections were incubated for 2 h with the peroxidase-conjugated donkey anti-goat IgG Fab fragment (Jackson ImmunoResearch Laboratories, West Grove, PA, USA) diluted 1:100 in PBS. After being rinsed with Tris–HCl buffer, the sections were exposed to a mixture of 0.05% 3,3′-diaminobenzidine and 0.01% H_2O_2 for 5 min at room temperature. The sections were dehydrated with graded ethanol and xylene, mounted in Permount, and examined by light microscope.

2.8 PI(3)P mass strip assay

Extraction, detection, and quantification of PI(3)P were performed with a PI(3)P Mass Strip Kit (Echelon Biosciences, Inc., Salt Lake City, UT, USA), according to the manufacturer's instructions. After extraction of neutral and acidic lipids and phase split step, the organic (lower) phase was transferred and dried in a vacuum dryer. Dried lipid samples were reconstituted and spotted onto a PI(3)P strip. Primary and secondary PI(3)P detector solutions were added sequentially to this strip. Finally, PI(3)P was detected with a chemiluminescent developing solution and visualized with the LAS-3000.

2.9 Chemicals

Cells were loaded with Gb3 (Matreya, Pleasant Gap, PA, USA) by incubating the cells in Gb3-added culture medium at 37°C or by adding Gb3 to the pipette solution at the concentration of 5 or 15 μmol/L. PI(3)P (#P-3016; Echelon Biosciences, Inc.,) was applied to the pipette solution at 100 nmol/L. TRAM-34 (Sigma-Aldrich, St Louis, MO, USA) and 1-EBIO (Tocris Bioscience, Ellisville, MO, USA) were applied to the bath solution at 10 and 100 μmol/L, respectively. Gb3, TRAM-34, and 1-EBIO were dissolved in DMSO, and PI(3)P were dissolved in 1:2:0.8 $CHCl_3$:MeOH:H_2O.

2.10 Statistical analysis

Pooled data are given as mean ± SEM. Statistical evaluation of data was performed by Student's *t*-test or ANOVA Tukey's test. Values of $P < 0.05$ were considered significant: $^*P < 0.05$ vs. control.

3. Results

3.1 $K_{Ca}3.1$ current and the channel expression are markedly reduced in aged Gla knockout mice

We first compared age-dependent changes in the $K_{Ca}3.1$ current in MAECs isolated from wild-type and *Gla* knockout mice. In the whole-cell patch-clamp configuration, an outward current was activated by loading cells with 1 μmol/L Ca^{2+} in the patch pipette (*Figure 1*). The current/voltage (*I*/*V*) curve produced by ramp pulses was linear at potentials negative to +50 mV and bent towards an abscissa at potentials positive to +50 mV. This Ca^{2+}-activated current was further augmented by the $K_{Ca}3.1$ channel activator 1-EBIO and completely inhibited by the $K_{Ca}3.1$ channel-specific inhibitor TRAM-34. These data suggest that the activated current is $K_{Ca}3.1$ current. No significant difference of current density at +50 mV was observed in MAECs from 4-week-old, 20-week-old, and 36-week-old wild-type mice (*Figure 1A*, *B* and *E*), whereas the current density was significantly reduced by 45.3 and 80.3%, respectively, in MAECs from 20-week-old and 28-week-old *Gla* knockout mice when compared with the current density in MAECs from 4-week-old *Gla* knockout mice (*Figure 1C–E*). In contrast, there was no significant difference in current densities between 4-week-old wild-type and *Gla* knockout mice (*Figure 1F*). These data suggest that $K_{Ca}3.1$ current densities are significantly decreased in an age-dependent manner in *Gla* knockout MAECs but not in wild-type MAECs.

Since down-regulation of the $K_{Ca}3.1$ channel may reduce the current, mRNA expression of the gene encoding the $K_{Ca}3.1$ channel (*Kcnn4*) and the channel protein expression were compared in MAECs isolated from age-matched wild-type and *Gla* knockout mice using real-time PCR (*Figure 2A*), immunocytochemistry (*Figure 2B*), and immunoblot analysis (*Figure 2C*). Their expressions were not changed age-dependently in wild-type MAECs, whereas the expressions were significantly reduced in aged *Gla* knockout MAECs. In addition, we further examined the $K_{Ca}3.1$ channel expression *in vivo*. Compared with wild-type (28-week-old), the $K_{Ca}3.1$ channel expression was markedly reduced in endothelial cells from aorta of age-matched *Gla* knockout mice (*Figure 2D*).

In *Gla* knockout mice, Gb3 accumulates in various types of cells, including endothelial cells, in an age-dependent manner. Thus, we hypothesized that the accumulated Gb3 reduces $K_{Ca}3.1$ current and the channel expression in aged *Gla* knockout mice.

3.2 Exogenously added Gb3 inhibits $K_{Ca}3.1$ current and channel expression

To test the hypothesis, we examined whether exogenously added Gb3 reduces $K_{Ca}3.1$ current in MAECs. Gb3 was added to the culture media, and cells were incubated for 2 h. $K_{Ca}3.1$ current then was activated by loading MAECs with 2 μmol/L Ca^{2+} via the patch pipette, and further activated by 1-EBIO. The $K_{Ca}3.1$ current was significantly decreased by incubation with Gb3. When compared with the vehicle-treated control, exposure to 5 or 15 μmol/L Gb3 reduced current density at +50 mV by 30.0 and 56.7%, respectively (*Figure 3A* and *B*). These results suggest that exogenously added Gb3 inhibits $K_{Ca}3.1$ current in a concentration-dependent manner. In addition, we examined whether exogenously added Gb3 reduces $K_{Ca}3.1$ channel expression in MAECs. mRNA and protein expression of $K_{Ca}3.1$ channel were significantly reduced in Gb3-treated cells in a concentration-dependent manner (*Figure 3C–E*), consistent with the results from age-matched wild-type and *Gla* knockout mice.

3.3 Gb3 down-regulates the $K_{Ca}3.1$ channel by inhibiting ERK/AP-1 pathway and up-regulating REST

To further evaluate the molecular mechanisms of $K_{Ca}3.1$ channel down-regulation by Gb3, we examined whether Gb3 could affect the signal transduction pathways related to $K_{Ca}3.1$ channel expression, the ERK/AP-1 pathway,[8] and REST.[16] The binding of nuclear extract to synthetic oligonucleotides containing an AP-1

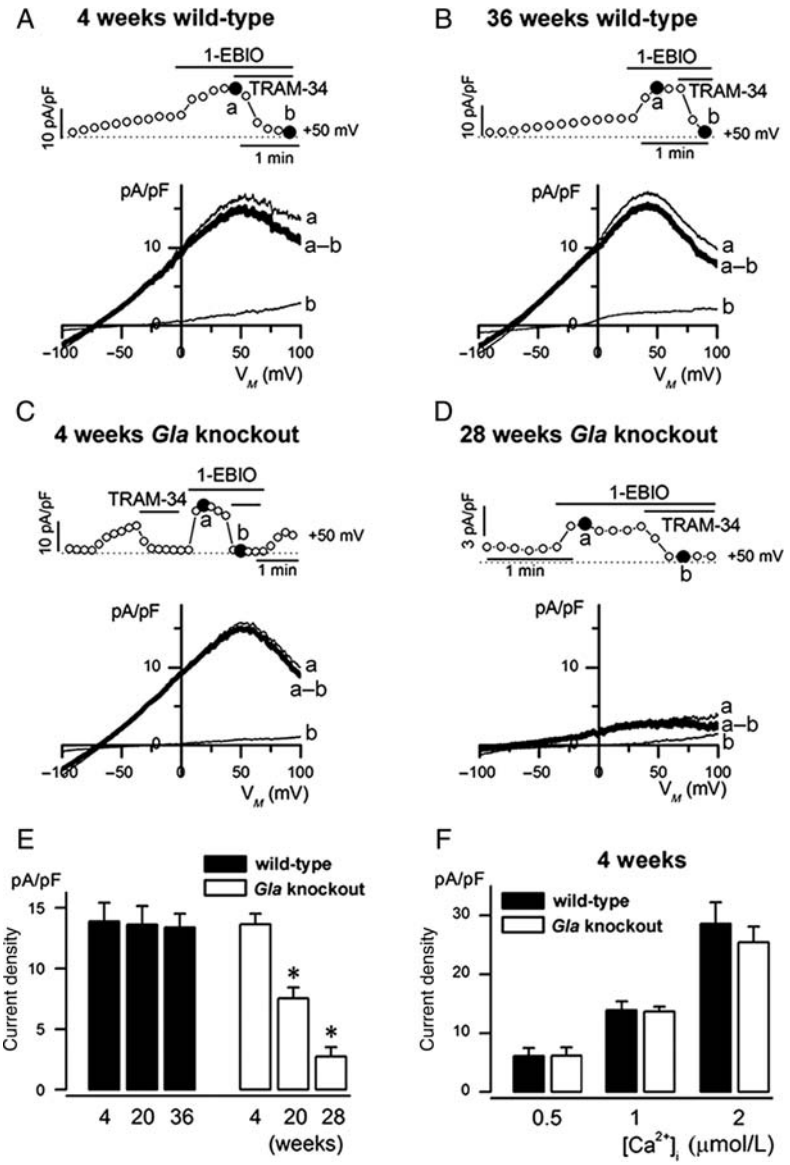

Figure 1 Decrease of K_{Ca}3.1 current in aged *Gla* knockout mouse aortic endothelial cells (MAECs). (*A*–*D*) Current densities (upper panels) are shown at a membrane potential of +50 mV (circles), and *I/V* relationships (lower panels) were obtained at the points marked by closed circles of the upper panels. (*E*) Summary of K_{Ca}3.1 current densities at +50 mV in wild-type (black bars; $n = 9$–12) and *Gla* knockout MAECs (white bars; $n = 9$–13). (*F*) Current densities at +50 mV against $[Ca^{2+}]_i$ were compared between 4-week-old wild-type and *Gla* knockout MAECs. Bar graphs represent mean ± SEM. $^*P < 0.05$ vs. 4-week-old wild-type MAECs.

consensus sequence was inhibited in Gb3-treated (*Figure 4A*) and aged *Gla* knockout MAECs (*Figure 4B*), suggesting that Gb3 can specifically inhibit AP-1 DNA-binding activity. The prominent decrease of AP-1 DNA-binding activity was detected at 15 min after Gb3 treatment, and activity was further decreased with an increase in treatment duration of up to 1 h (data not shown). To investigate whether Gb3 mediates AP-1 via mitogen-activated protein kinase (MAPK)-signalling pathways, we assessed the phosphorylation of ERK1/2 (p-ERK1/2) by immunoblot analysis. p-ERK1/2 levels were significantly reduced in Gb3-treated (*Figure 4C*) and aged *Gla* knockout MAECs (*Figure 4D*). In addition, mRNA expression of REST was significantly up-regulated in Gb3-treated (*Figure 4E*) and aged *Gla* knockout MAECs (*Figure 4F*). These data suggest that the accumulated Gb3 down-regulates K_{Ca}3.1 channel by inhibiting the ERK/AP-1 pathway and up-regulating REST in Gb3-treated and aged *Gla* knockout MAECs.

3.4 Gb3 inhibits K_{Ca}3.1 current by decreasing intracellular levels of PI(3)P

In addition to down-regulation of the K_{Ca}3.1 channel, Gb3-induced reduction in K_{Ca}3.1 current may be evoked by the decrease in K_{Ca}3.1 channel activity. K_{Ca}3.1 channel was reported to be activated by PI(3)P,[17,18] which is produced by PI3K from phosphatidylinositol. Among the PI3K classes, class III produces only PI(3)P. Therefore, we assessed the changes of class III PI3K by Gb3. Class III PI3K

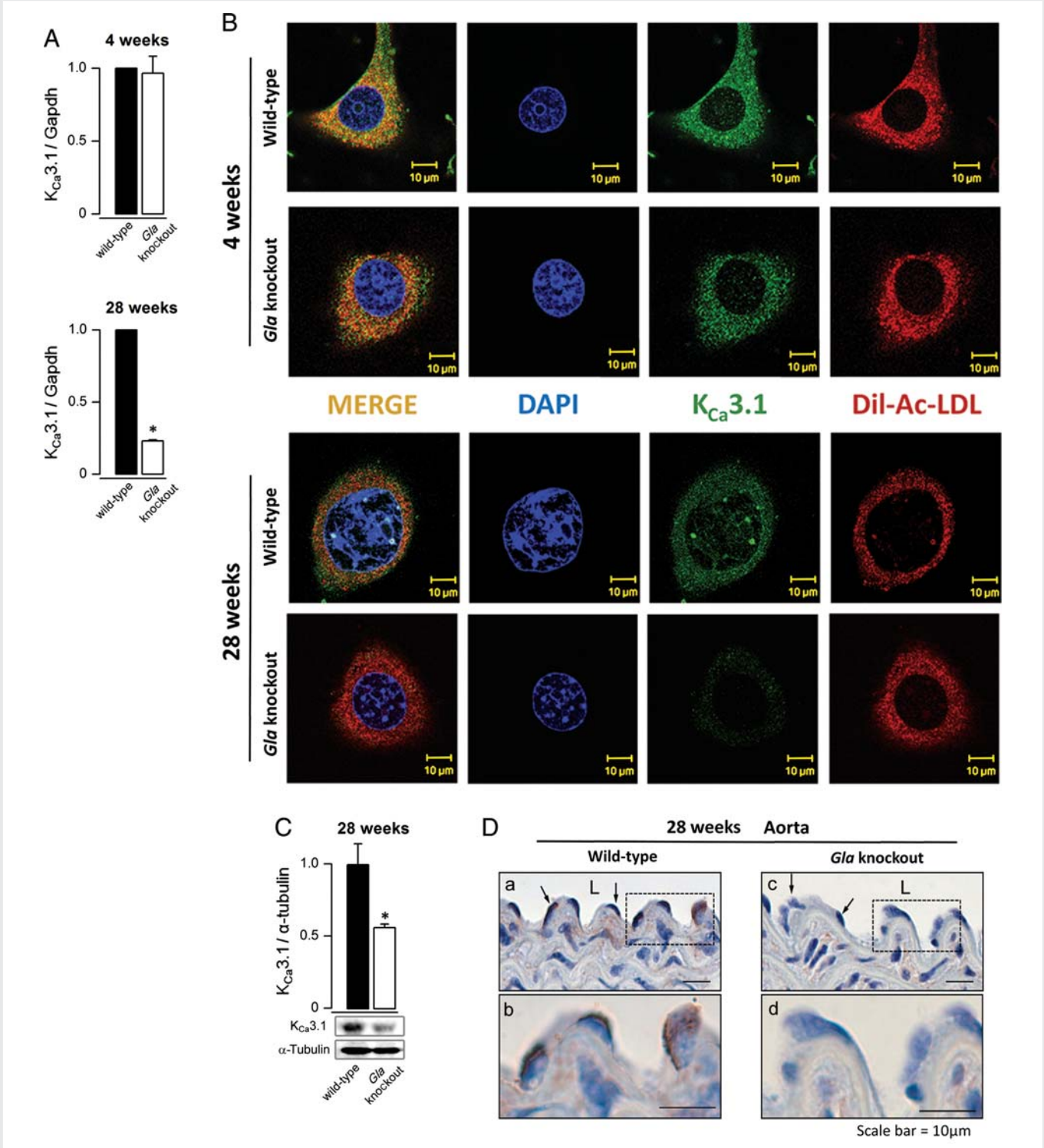

Figure 2 Down-regulation of K_{Ca}3.1 channel in aged *Gla* knockout MAECs. (*A*–*C*) K_{Ca}3.1 channel mRNA and protein expressions were compared in MAECs isolated from age-matched wild-type and Gla knockout mice using real-time PCR (*A*), immunocytochemistry (*B*), and immunoblot analysis (*C*). Relative mRNA and protein levels were expressed as a ratio of the age-matched wild-type MAECs ($n = 3$–7). Immunocytochemistry shows K_{Ca}3.1 channel labelling (green), uptaked DiI-Ac-LDL fluorescence (red) and nuclear staining with DAPI (blue); combined images are also presented. *$P < 0.05$ vs. age-matched wild-type MAECs. (*D*) *In vivo* localization of K_{Ca}3.1 channel protein in aorta from 28-week-old wild-type (a and b) and age-matched *Gla* knockout mice (c and d). 'L' indicates lumen. Enlargements of black boxes (dotted line) in a and c were shown in b and d, respectively. $n = 3$ per experimental paradigm.

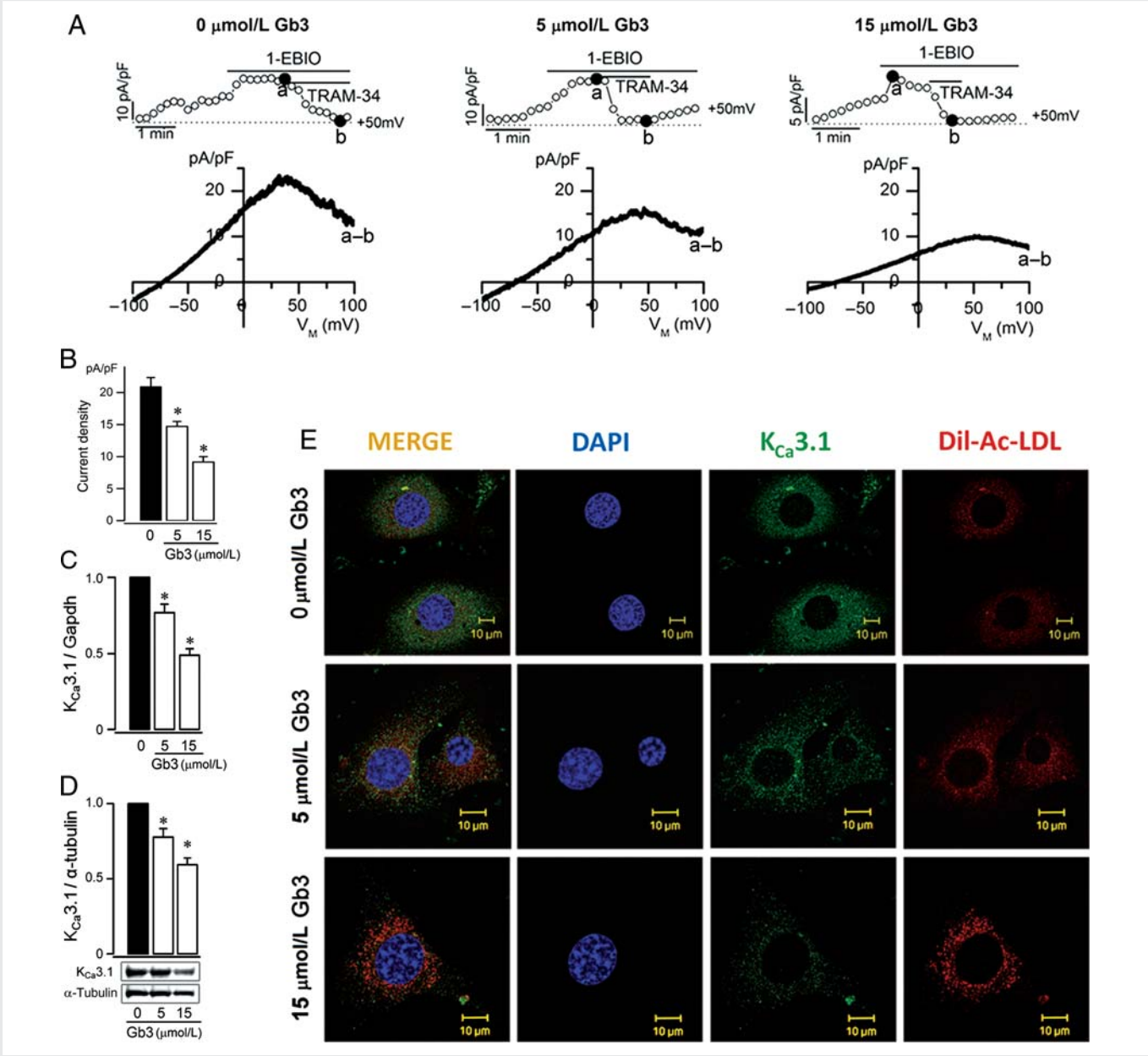

Figure 3 Decrease of K_{Ca}3.1 current and the channel expression in Gb3-treated MAECs. (*A*) Current densities (upper panels) are shown at a membrane potential of +50 mV (circles), and I/V relationships (lower panels) were obtained at the points marked by closed circles of the upper panels. (*B*) Summary of K_{Ca}3.1 current densities at +50 mV in MAECs ($n = 4–7$). (*C–E*) K_{Ca}3.1 channel mRNA and protein expressions were measured using real-time PCR (*C*), immunoblot (*D*) and immunocytochemistry (*E*). Relative mRNA and protein levels were expressed as a ratio of the vehicle-treated control. Immunocytochemistry shows K_{Ca}3.1 labelling (green), uptaked DiI-Ac-LDL fluorescence (red) and nuclear staining with DAPI (blue); combined images are also presented. *$P < 0.05$ vs. vehicle-treated control.

expression was decreased in both Gb3-treated (*Figure 5A*) and aged *Gla* knockout MAECs (*Figure 5B*). Furthermore, intracellular levels of PI(3)P were significantly decreased by Gb3, suggesting that Gb3 reduces K_{Ca}3.1 channel activity by decreasing intracellular levels of PI(3)P (*Figure 5C*). Next, we examined whether PI(3)P recovers the K_{Ca}3.1 current reduced by Gb3 (*Figure 5D*). Gb3 and PI(3)P was applied to MAECs via the patch pipette. K_{Ca}3.1 current was decreased by Gb3 in a concentration-dependent manner and the decreased current was recovered by PI(3)P ($n = 4$). Furthermore, PI(3)P restored the reduced K_{Ca}3.1 current in aged *Gla* knockout MAECs ($n = 4$; *Figure 5E*). These results suggest that Gb3 can inhibit K_{Ca}3.1 channel activity by decreasing intracellular levels of PI(3)P.

We then evaluated whether Gb3 directly changes the gating properties of the K_{Ca}3.1 channel. Single-channel recording was performed using inside-out membrane patches. Gb3 (15 μmol/L) did not change open probability, open-time distribution, and single-channel conductance of the channel (data not shown), suggesting that Gb3 does not change the gating properties of the K_{Ca}3.1 channel directly.

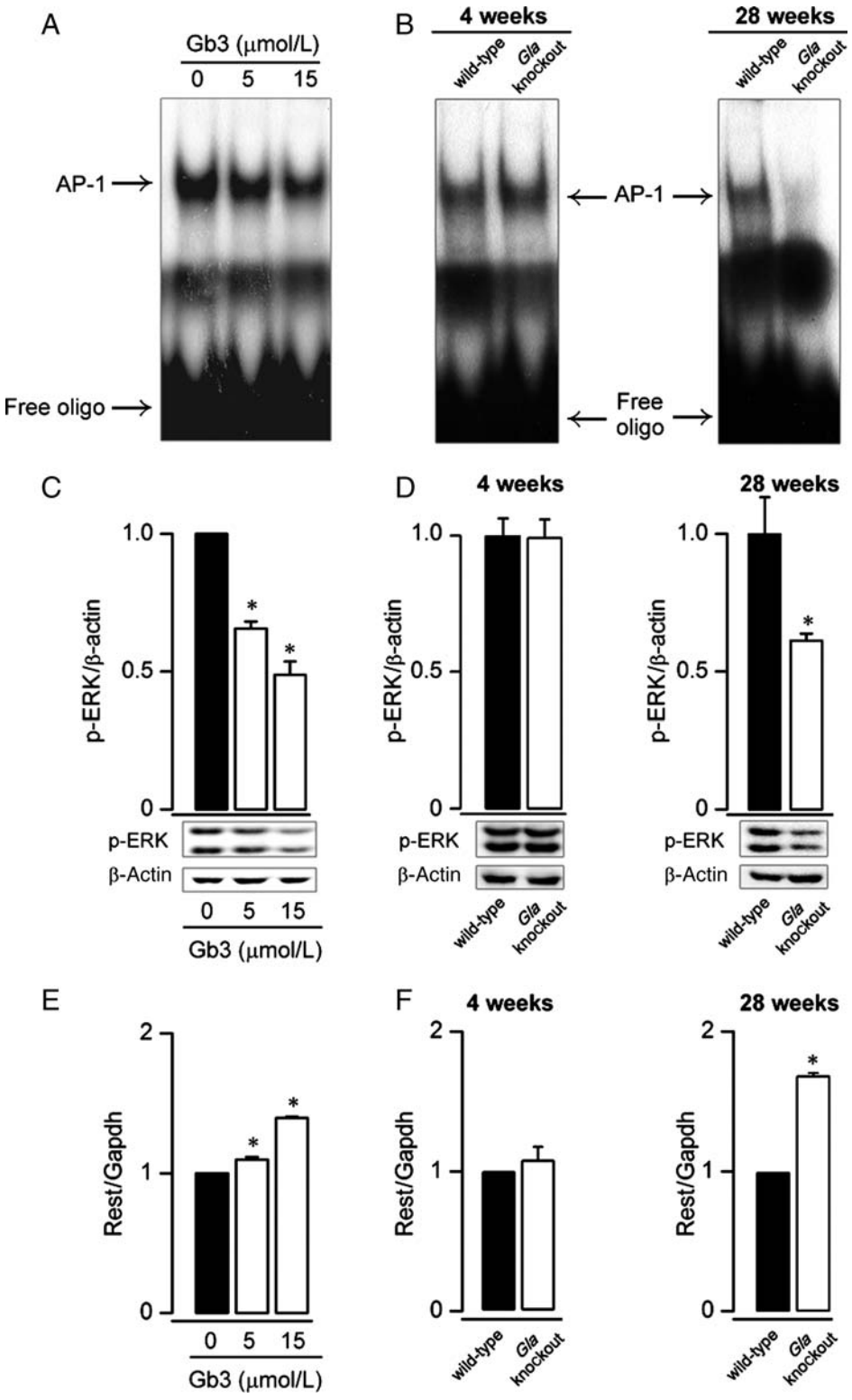

Figure 4 ERK/AP-1 pathway and REST regulation in Gb3-treated or aged *Gla* knockout MAECs. The levels of AP-1, p-ERK and REST were compared in MAECs incubated in Gb3-containing culture media (*A*: for 1 h, *C* and *E*: for 2 h) or in MAECs isolated from age-matched wild-type and Gla knockout mice (*B*, *D*, and *F*) using EMSA (*A* and *B*), western blotting (*C* and *D*) and real-time PCR (*E* and *F*), respectively. (*A*–*B*) Down-regulation of AP-1 in Gb3-treated (*A*) and aged *Gla* knockout MAECs (*B*). The upper arrow indicates complexes of AP-1, and the lower arrow the labelled oligonucleotide. (*C*–*D*) Down-regulation of p-ERK in Gb3-treated (*C*) and age-matched *Gla* knockout MAECs (*D*). (*E*–*F*) Up-regulation of REST. Relative protein or mRNA levels were expressed as a ratio of the vehicle-treated control or age-matched wild-type MAECs. $^*P < 0.05$ vs. vehicle-treated control (*C* and *E*) or age-matched wild-type MAECs (*D* and *F*).

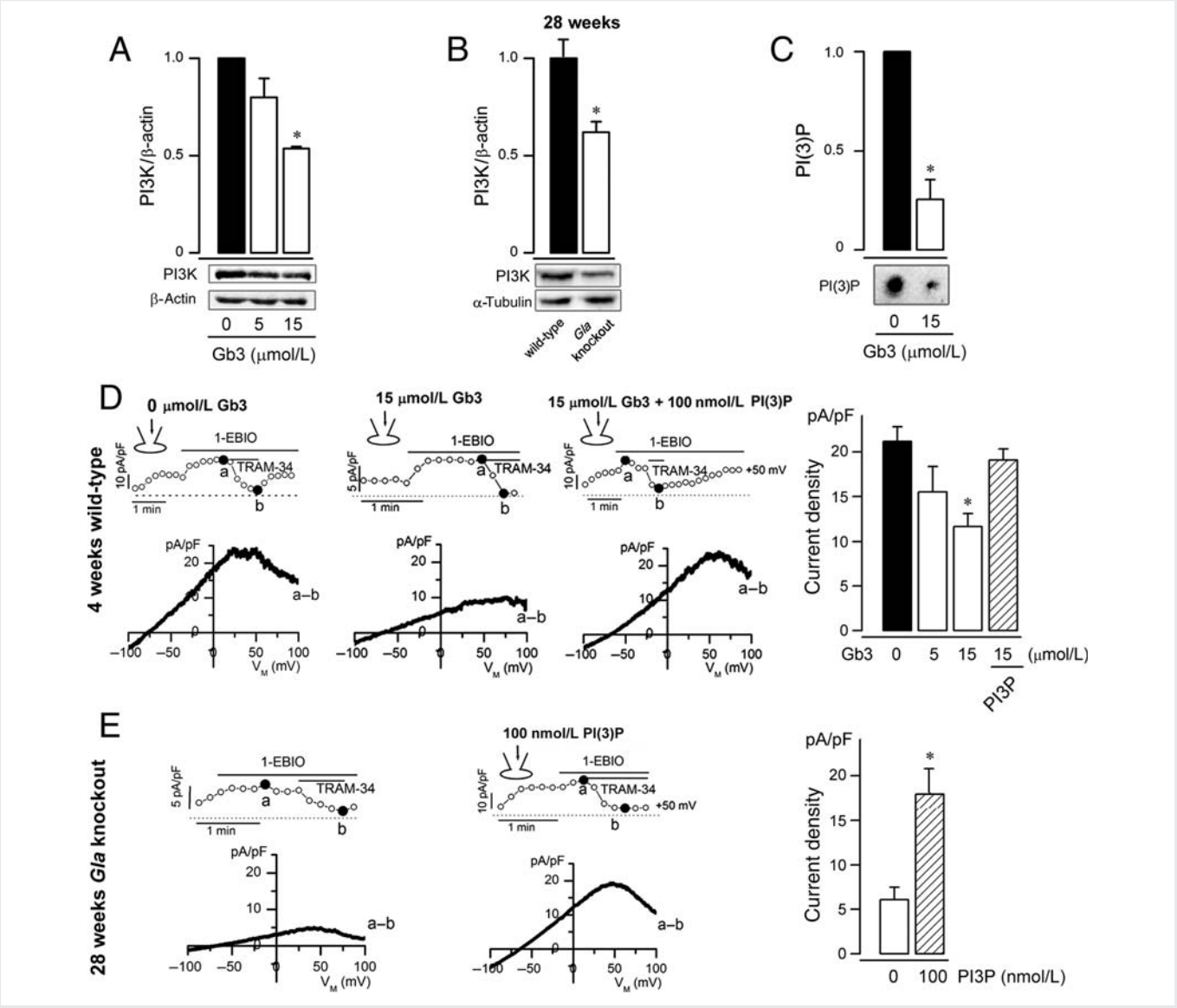

Figure 5 Gb3-induced PI(3)P decrease and K_{Ca}3.1 current inhibition (*A* and *B*) Expression of class III PI3K was tested by immunoblot in MAECs incubated with Gb3-containing culture media for 2 h (*A*) or in MAECs isolated from 28-week-old wild-type and *Gla* knockout mice (*B*). β-actin or α-tubulin was used to assess equal loading of the samples. (*C*) Representative PI(3)P strip. PI(3)P was extracted and detected using a PI(3)P Mass Strip Kit. (*D* and *E*) K_{Ca}3.1 current was activated by 2 μmol/L $[Ca^{2+}]_i$. Gb3, PI(3)P or Gb3 plus PI(3)P was applied to 4-week-old wile-type (*D*) or 28-week-old *Gla* knockout MAEC (*E*) via the patch pipette. Current densities are shown at a membrane potential of +50 mV (circles), and I/V relationships were obtained at the points marked by closed circles. Summary of K_{Ca}3.1 current densities at +50 mV ($n = 3–5$) is presented on the right panel. *$P < 0.05$ vs. vehicle-treated control (*A*, *C*, and *D*) or 28-week-old wild-type MAECs (*B*) or 28-week-old *Gla* knockout MAECs (*E*).

3.5 Exogenously added Gb3 inhibits EDR of wild-type mouse aortic rings

It was reported that EDR to ACh was significantly attenuated in vessels from *Gla* knockout mice.[5,6] However, it is still unknown whether the impaired EDR in *Gla* knockout mice is related to the K_{Ca}3.1 channel inhibition by Gb3. Thus, we examined whether exogenously added Gb3 inhibits EDR. Since vascular smooth muscle contraction to U46619 was not blunted in *Gla* knockout mice,[5,6] isolated mouse aortic ring from wild-type mice was contracted by U46619 (1 μmol/L) and then EDR was evoked by ACh (1 μmol/L). TRAM-34 (10 μmol/L) partially inhibited ACh-induced EDR in endothelium-intact aortic rings (*Figure 6A*). On the other hand, U46619-induced contraction was not changed by TRAM-34 in endothelium-denuded aortic rings (*Figure 6B*). These results suggest that K_{Ca}3.1 channel inhibition impairs EDR. Then we examined the effect of Gb3 on EDR (*Figure 6C–E*). Precontracted endothelium-intact aortic ring was relaxed by ACh in a concentration-dependent manner (*Figure 6D* and *E*) and ACh-induced EDR was maintained up to 500 s after ACh application (*Figure 6C*). In contrast, when the aortic ring was treated by Gb3 (15 μmol/L) for 2 h, ACh-induced EDR was decreased in magnitude (*Figure 6D* and *E*) and not maintained for such a long time (*Figure 6C*). The relaxed aortic ring was re-contracted with time in

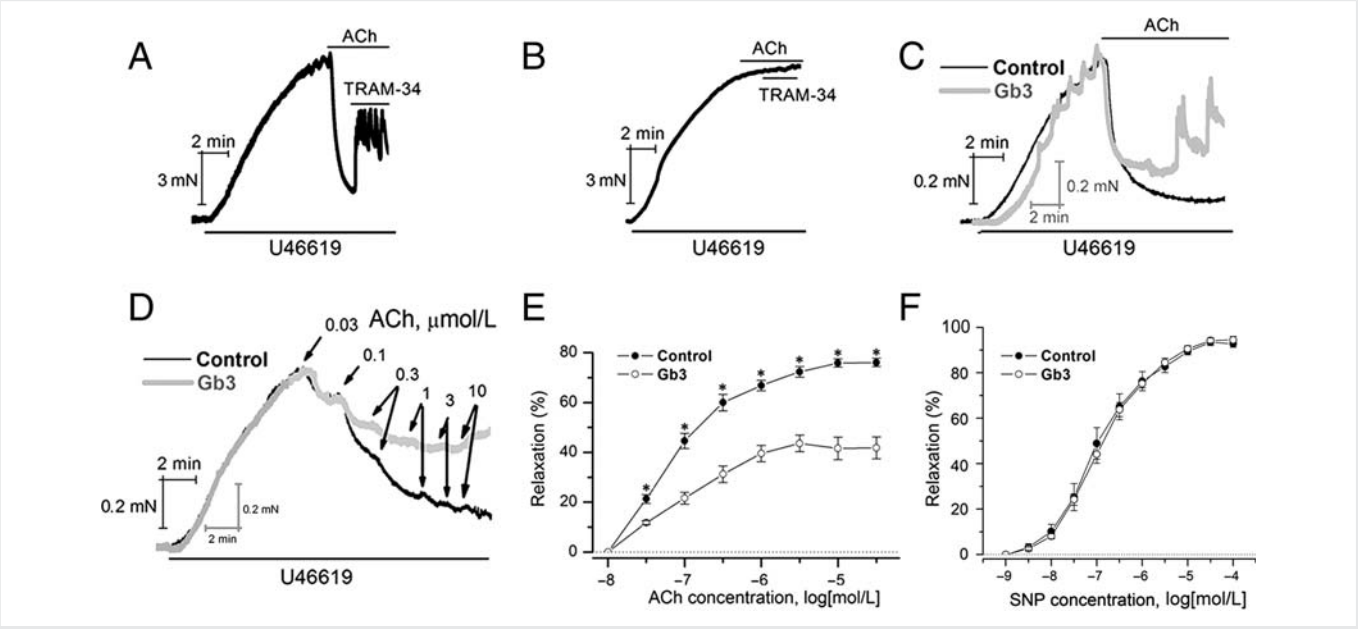

Figure 6 Effect of the $K_{Ca}3.1$ channel inhibitor TRAM-34 and Gb3 on ACh-induced EDR Mouse aortic rings were exposed to Gb3 by perfusing rings with Gb3 (15 μmol/L)-contraining Krebs/Ringer bicarbonate solution for 2 h (*C*–*E*). (*A*) ACh-induced EDR was partially inhibited by the $K_{Ca}3.1$ channel blocker TRAM-34. (*B*) Effect of TRAM-34 on the contraction of endothelium-denuded mouse aortic ring. (*C*) Effect of Gb3 on ACh-induced EDR. EDR was evoked by 1 μmol/L ACh in control (black line) and Gb3-incubated aortic ring (gray line). (*D*) A concentration-dependent ACh-induced EDR in control (black line) and Gb3-incubated aortic ring (gray line). (*E* and *F*) Summary ($n = 6$) of vasorelaxation by ACh (*E*) or sodium nitroprusside (*F*) in control (closed circle) and Gb3-incubated aortic ring (open circle). Sodium nitroprusside-induced relaxation was measured in endothelium-denuded aortic rings. The magnitude of relaxation at each treatment was expressed as a percentage of initial U46619-induced contraction. *$P < 0.05$ vs. control.

spite of the presence of ACh. We, then, examined whether Gb3 affects nitrovasodilator-induced relaxation in endothelium-denuded aortic rings (*Figure 6F*). Precontracted aortic ring was relaxed by sodium nitroprusside in a concentration-dependent manner and sodium nitroprusside-induced relaxation was not changed by Gb3 (15 μmol/L) treatment for 2 h, suggesting that Gb3 does not affect the reactivity to NO of vascular smooth muscle. These results suggest that EDR is attenuated by $K_{Ca}3.1$ channel inhibition and Gb3.

4. Discussion

We have shown that Gb3 modulates $K_{Ca}3.1$ channel in MAECs of aged *Gla* knockout mice and Gb3-treated MAECs by decreasing the protein expression and the channel activity. Gb3-induced down-regulation of p-ERK and AP-1 and up-regulation of REST lead to a decrease in $K_{Ca}3.1$ channel expression. In addition, the Gb3-induced decrease in intracellular PI(3)P concentrations reduces the $K_{Ca}3.1$ current in Gb3-treated and aged *Gla* knockout MAECs. These findings represent the first direct evidence for the underlying mechanisms of Gb3-induced $K_{Ca}3.1$ channel dysfunction, which may be implicated in the endothelial dysfunction of Fabry disease.

These results were obtained by measuring $K_{Ca}3.1$ channel expression and activity in both *Gla* knockout and Gb3-treated MAECs. In the course of these two measurements, $K_{Ca}3.1$ channel dysfunction was observed quite consistently, with similar channel dysfunction observed in both aged *Gla* knockout and Gb3-treated MAECs. In *Gla* knockout mice, Gb3 was accumulated in endothelial cells, which plateaued at 12 to 16 weeks.[19] Therefore, Gb3 may be saturated in endothelial cells of 28-week-old *Gla* knockout mice. In addition, since the plasma concentration of Gb3 ranges from 6.7 to 15.4 μmol/L in patients with classic Fabry disease,[20] the Gb3 concentration used in this study (up to 15 μmol/L) is within the range observed in Fabry disease. Therefore, we suggest that accumulated Gb3 evokes $K_{Ca}3.1$ channel dysfunction in *Gla* knockout mice.

The present study shows that Gb3 induces a rapid down-regulation of $K_{Ca}3.1$ channel protein. The mechanism for this might be due to defective synthesis, since Gb3 inhibited ERK/AP-1 pathway and up-regulated REST. However, a rapid down-regulation of the channel protein suggests another possibility. As shown in HERG channel,[9,21] a rapid down-regulation of the channel protein could be caused by internalization and increased degradation of the channel. Thus, further studies are required to distinguish whether Gb3 facilitates internalization and degradation of the channel.

In the previous research, we suggested reactive oxygen species (ROS) inhibit ERK 1/2 phosphorylation in human endothelial cells,[22] and it is already reported that Gb3 induces ROS generation in endothelial cells.[23] Therefore, ROS produced by Gb3 accumulation could down-regulate p-ERK, resulting in the inhibition of $K_{Ca}3.1$ channel expression. However, the effect of ROS on ERK is still controversial, since ROS-induced ERK activation was also reported.[24] The modulation of ERK pathway by Gb3 needs to be clarified in detail.

Since inhibition of ERK or PI3K can suppress eNOS expression,[22,25] down-regulated p-ERK and PI3K by Gb3 could contribute to the impaired EDR by reduction in NO production. In addition, REST also affects EDR via $K_{Ca}3.1$ channel modulation, since augmented

REST decreased K_{Ca}3.1 channel expression. In fact, K_{Ca}3.1 channels in endothelial cells regulate Ca^{2+} influx, thereby determining EDR.[7] Thus K_{Ca}3.1 channel dysfunction impairs EDR. Therefore, impaired EDR found in *Gla* knockout mice may be caused by various mechanisms: PI3K inhibition, p-ERK down-regulation, REST up-regulation, or K_{Ca}3.1 channel dysfunction. According to recent researches using K_{Ca}3.1 knockout mice,[26,27] K_{Ca}3.1 deficiency has a severe impact on ACh-induced EDR, resulting in the significant increase in arterial blood pressure. These results could explain uncontrolled hypertension in Fabry patients.[28]

Since endothelium-independent relaxation was normal in the aorta from *Gla* knockout mice,[6] Gb3 seems to have no effect on vascular smooth muscles. This might be, at least partially, explained by the absence of Gb3 effect on K_{Ca}1.1 channel. K_{Ca}1.1 channel, known as large-conductance Ca^{2+}-activated K^+ channel, is expressed in mouse aortic smooth muscle cells.[29] K_{Ca}1.1 current and the channel expression were not affected by Gb3 (data not shown), suggesting that Gb3 might have no effect on K_{Ca}1.1 channel.

In conclusion, the identification of the K_{Ca}3.1 channel as a target for Gb3 raises important questions about the contribution of this interaction to the process of Fabry disease. The K_{Ca}3.1 channel is expressed in various cells, including endothelial cells, fibroblasts, proliferating smooth muscle cells, microglia, and lymphocytes.[30] Given the significant role of the K_{Ca}3.1 channel in the cellular functions of these cells, it is noteworthy that the Gb3 content of cells, including endothelial cells, can be correlated with the progress of Fabry disease. Thus, K_{Ca}3.1 is a potential therapeutic target for the disease.

Conflict of interest: none declared.

Funding

This work was supported by the Korea Research Foundation Grant funded by the Korea Government (MOEHRD) (KRF-2008–041-E00028).

References

1. Brady RO, Gal AE, Bradley RM, Martensson E, Warshaw AL, Laster L. Enzymatic defect in Fabry's disease. Ceramidetrihexosidase deficiency. *N Engl J Med* 1967;**276**:1163–1167.
2. Zarate YA, Hopkin RJ. Fabry's disease. *Lancet* 2008;**372**:1427–1435.
3. Branton MH, Schiffmann R, Sabnis SG, Murray GJ, Quirk JM, Altarescu G *et al*. Natural history of Fabry renal disease: influence of alpha-galactosidase A activity and genetic mutations on clinical course. *Medicine (Baltimore)* 2002;**81**:122–138.
4. Linhart A, Kampmann C, Zamorano JL, Sunder-Plassmann G, Beck M, Mehta A *et al*. Cardiac manifestations of Anderson-Fabry disease: results from the international Fabry outcome survey. *Eur Heart J* 2007;**28**:1228–1235.
5. Shu L, Park JL, Byun J, Pennathur S, Kollmeyer J, Shayman JA. Decreased nitric oxide bioavailability in a mouse model of Fabry disease. *J Am Soc Nephrol* 2009;**20**:1975–1985.
6. Park JL, Whitesall SE, D'Alecy LG, Shu L, Shayman JA. Vascular dysfunction in the alpha-galactosidase A-knockout mouse is an endothelial cell-, plasma membrane-based defect. *Clin Exp Pharmacol Physiol* 2008;**35**:1156–1163.
7. Ahn SC, Seol GH, Kim JA, Suh SH. Characteristics and a functional implication of Ca^{2+}-activated K^+ current in mouse aortic endothelial cells. *Pflugers Arch* 2004;**447**:426–435.
8. Tharp DL, Bowles DK. The intermediate-conductance Ca^{2+}-activated K^+ channel (K_{Ca}3.1) in vascular disease. *Cardiovasc Hematol Agents Med Chem* 2009;**7**:1–11.
9. Chapman H, Ramstrom C, Korhonen L, Laine M, Wann KT, Lindholm D *et al*. Down-regulation of the HERG (KCNH2) K^+ channel by ceramide: evidence for ubiquitin-mediated lysosomal degradation. *J Cell Sci* 2005;**118**:5325–5334.
10. Titievsky A, Titievskaya I, Pasternack M, Kaila K, Tornquist K. Sphingosine inhibits voltage-operated calcium channels in GH4C1 cells. *J Biol Chem* 1998;**273**:242–247.
11. Jung SC, Han IP, Limaye A, Xu R, Gelderman MP, Zerfas P *et al*. Adeno-associated viral vector-mediated gene transfer results in long-term enzymatic and functional correction in multiple organs of Fabry mice. *Proc Natl Acad Sci U S A* 2001;**98**:2676–2681.
12. Suh SH, Vennekens R, Manolopoulos VG, Freichel M, Schweig U, Prenen J *et al*. Characterisation of explanted endothelial cells from mouse aorta: electrophysiology and Ca^{2+} signalling. *Pflugers Arch* 1999;**438**:612–620.
13. Manolopoulos VG, Liu J, Unsworth BR, Lelkes PI. Adenylyl cyclase isoforms are differentially expressed in primary cultures of endothelial cells and whole tissue homogenates from various rat tissues. *Biochem Biophys Res Commun* 1995;**208**:323–331.
14. Nilius B, Schwartz G, Oike M, Droogmans G. Histamine-activated, non-selective cation currents and Ca^{2+} transients in endothelial cells from human umbilical vein. *Pflugers Arch* 1993;**424**:285–293.
15. Lauf PK, Misri S, Chimote AA, Adragna NC. Apparent intermediate K conductance channel hyposmotic activation in human lens epithelial cells. *Am J Physiol Cell Physiol* 2008;**294**:C820–832.
16. Cheong A, Bingham AJ, Li J, Kumar B, Sukumar P, Munsch C *et al*. Downregulated REST transcription factor is a switch enabling critical potassium channel expression and cell proliferation. *Mol Cell* 2005;**20**:45–52.
17. Srivastava S, Li Z, Lin L, Liu G, Ko K, Coetzee WA *et al*. The phosphatidylinositol 3-phosphate phosphatase myotubularin-related protein 6 (MTMR6) is a negative regulator of the Ca^{2+}-activated K^+ channel K_{Ca}3.1. *Mol Cell Biol* 2005;**25**:3630–3638.
18. Srivastava S, Choudhury P, Li Z, Liu G, Nadkarni V, Ko K *et al*. Phosphatidylinositol 3-phosphate indirectly activates K_{Ca}3.1 via 14 amino acids in the carboxy terminus of K_{Ca}3.1. *Mol Biol Cell* 2006;**17**:146–154.
19. Shu L, Murphy HS, Cooling L, Shayman JA. An *in vitro* model of Fabry disease. *J Am Soc Nephrol* 2005;**16**:2636–2645.
20. von Scheidt W, Eng CM, Fitzmaurice TF, Erdmann E, Hubner G, Olsen EG *et al*. An atypical variant of Fabry's disease with manifestations confined to the myocardium. *N Engl J Med* 1991;**324**:395–399.
21. Guo J, Massaeli H, Xu J, Jia Z, Wigle JT, Mesaeli N *et al*. Extracellular K^+ concentration controls cell surface density of IKr in rabbit hearts and of the HERG channel in human cell lines. *J Clin Invest* 2009;**119**:2745–2757.
22. Choi S, Park S, Liang GH, Kim JA, Suh SH. Superoxide generated by lysophosphatidylcholine induces endothelial nitric oxide synthase downregulation in human endothelial cells. *Cell Physiol Biochem* 2010;**25**:233–240.
23. Shen JS, Meng XL, Moore DF, Quirk JM, Shayman JA, Schiffmann R *et al*. Globotriaosylceramide induces oxidative stress and up-regulates cell adhesion molecule expression in Fabry disease endothelial cells. *Mol Genet Metab* 2008;**95**:163–168.
24. Samavati L, Monick MM, Sanlioglu S, Buettner GR, Oberley LW, Hunninghake GW. Mitochondrial K_{ATP} channel openers activate the ERK kinase by an oxidant-dependent mechanism. *Am J Physiol Cell Physiol* 2002;**283**:C273–C281.
25. Merla R, Ye Y, Lin Y, Manickavasagam S, Huang MH, Perez-Polo RJ *et al*. The central role of adenosine in statin-induced ERK1/2, Akt, and eNOS phosphorylation. *Am J Physiol Heart Circ Physiol* 2007;**293**:H1918–H1928.
26. Si H, Heyken WT, Wolfle SE, Tysiac M, Schubert R, Grgic I *et al*. Impaired endothelium-derived hyperpolarizing factor-mediated dilations and increased blood pressure in mice deficient of the intermediate-conductance Ca^{2+}-activated K^+ channel. *Circ Res* 2006;**99**:537–544.
27. Brahler S, Kaistha A, Schmidt VJ, Wolfle SE, Busch C, Kaistha BP *et al*. Genetic deficit of SK3 and IK1 channels disrupts the endothelium-derived hyperpolarizing factor vasodilator pathway and causes hypertension. *Circulation* 2009;**119**:2323–2332.
28. Kleinert J, Dehout F, Schwarting A, de Lorenzo AG, Ricci R, Kampmann C *et al*. Prevalence of uncontrolled hypertension in patients with Fabry disease. *Am J Hypertens* 2006;**19**:782–787.
29. Liang GH, Kim JA, Seol GH, Choi S, Suh SH. The Na^+/Ca^{2+} exchanger inhibitor KB-R7943 activates large-conductance Ca^{2+}-activated K^+ channels in endothelial and vascular smooth muscle cells. *Eur J Pharmacol* 2008;**582**:35–41.
30. Wei AD, Gutman GA, Aldrich R, Chandy KG, Grissmer S, Wulff H. International Union of Pharmacology. LII. Nomenclature and molecular relationships of calcium-activated potassium channels. *Pharmacol Rev* 2005;**57**:463–472.